

Viphavakit, C., Atthi, N., Boonruang, S., Themistos, C., Mohammed, W. S., Kalli, K., Rahman, B. M. & Komodromos, M. (2014). Characterization of polymer nanowires fabricated using the nanoimprint method. Proceedings of SPIE, 9126, doi: 10.1117/12.2052276



**CITY UNIVERSITY  
LONDON**

[City Research Online](#)

**Original citation:** Viphavakit, C., Atthi, N., Boonruang, S., Themistos, C., Mohammed, W. S., Kalli, K., Rahman, B. M. & Komodromos, M. (2014). Characterization of polymer nanowires fabricated using the nanoimprint method. Proceedings of SPIE, 9126, doi: 10.1117/12.2052276

**Permanent City Research Online URL:** <http://openaccess.city.ac.uk/12216/>

#### **Copyright & reuse**

City University London has developed City Research Online so that its users may access the research outputs of City University London's staff. Copyright © and Moral Rights for this paper are retained by the individual author(s) and/ or other copyright holders. All material in City Research Online is checked for eligibility for copyright before being made available in the live archive. URLs from City Research Online may be freely distributed and linked to from other web pages.

#### **Versions of research**

The version in City Research Online may differ from the final published version. Users are advised to check the Permanent City Research Online URL above for the status of the paper.

#### **Enquiries**

If you have any enquiries about any aspect of City Research Online, or if you wish to make contact with the author(s) of this paper, please email the team at [publications@city.ac.uk](mailto:publications@city.ac.uk).

# Characterization of polymer nanowires fabricated using the nanoimprint method

Charusluk Viphavakit<sup>\*a</sup>, Nithi Atthi<sup>b</sup>, Sakoolkan Boonruang<sup>c</sup>, Christos Themistos<sup>a</sup>, Waleed S. Mohammed<sup>d</sup>, Kyriacos Kalli<sup>e</sup>, B.M.Azizur Rahman<sup>f</sup>, Michael Komodromos<sup>a</sup>

<sup>a</sup>Dept. of Electrical Engineering, Frederick University, 7 Frederickou Str., Nicosia, 1036, Cyprus;

<sup>b</sup>Thai Microelectronics Center (TMEC), Chachoengsao, 24000, Thailand; <sup>c</sup>Photonics Technology Laboratory, Thailand National Electronics and Computer Technology Center (NECTEC), Klong Luang, 10120, Pathumthani, Thailand; <sup>d</sup>Center of Research in Optoelectronics, Communication and Control System (BU-CROCCS), Bangkok University, Paholyotin Rd., Klong Luang, 10120, Pathumthani, Thailand; <sup>e</sup>Cyprus University of Technology, Kitiou Kiprianou str. 45, 3603 Limassol, Cyprus; <sup>f</sup>School of Engineering and Mathematical sciences, City University London, Room: C166, Northampton Square, London EC1V 0HB, UK

## ABSTRACT

In this paper, an ormocomp polymer nanowire with possible use in integrated-optics sensing applications is presented. We discuss the structure design, the fabrication process and present results of the simulation and characterization of the optical field profile. Since the nanowires are designed and intended to be used as integrated optics devices, they are attached to tapered and feed waveguides at their ends. The fabrication process in this work is based mainly on the nanoimprint technique. The method assumes a silicon nanowire as an original pattern, and polydimethylsiloxane (PDMS) as the soft mold. The PDMS mold is directly imprinted on the ormocomp layer and then cured by UV light to form the polymer based nanowire. The ormocomp nanowires are fabricated to have various dimensions of width and length at a fixed 500nm thickness. The length of the nanowires is varied from 250  $\mu\text{m}$  to 2 mm, whereas the width of the structures is varied between 500nm and 1 $\mu\text{m}$ . The possible optical mode field profile that occurs in the proposed polymer nanowire design is studied using the H-field finite element method (FEM). In the characterization part, the optical field profile and the intensity at the device output are the main focus of this paper. The various lengths of the nanowires show different characteristics in terms of output intensity. An image processing is used to process the image to obtain the intensity of the output signal. A comparison of the optical field and output intensity for each polymer nanowire is also discussed.

**Keywords:** Polymer nanowires, integrated optics, nanoimprint

## 1. INTRODUCTION

Nanowires have been a good candidate for nanotechnology applications due to their unique chemical and physical properties [1-3]. In the optics and photonics area, silicon-on-insulator (SOI) based nanowires are used as a waveguide in many sensing applications [4-8]. The SOI technology has been used in optical sensors because it has the advantage of improving the light confinement in the waveguide, thus sensitivity of the sensors is enhanced [9, 10]. However, polymer nanowires are alternatively used as optical waveguides nowadays in sensing applications due to their mechanical flexibility over the semiconductor nanowires such as silicon nanowires. The polymer nanowires are biocompatible materials which can have a various functional dopants [11, 12]. Therefore, they can be used in many different areas of sensing applications. For example, the polymer nanowires are used as chemical sensors, biosensors, organic light emitting diodes, and organic solar cells [13-16]. It has been reported that the polymer nanowire can be used in humidity sensing, and  $\text{NO}_2$  and  $\text{NH}_3$  detection with response time 30ms and high sensitivity [17]. The utility of fluorescent polymer nanofibers to detect the metal ions ( $\text{Fe}^{3+}$  and  $\text{Hg}^{2+}$ ) is also possible [18]. In this work, polymer based nanowires are proposed to detect the effective index difference when there is the change of refractive index of the cladding material.

\*charusluk.v@gmail.com

The sensing region of this polymer nanowire structure is at the interface between the guiding area and the cladding region where the evanescent wave takes place. In order to achieve a highly sensitive polymer nanowire the structure dimensions of width and height need to be optimized to enhance the power confinement in the sensing area. There are several methods to fabricate polymer nanowires, such as using electron beam lithography, electro-chemical deposition, anodic aluminum oxide, nanosphere lithography, and nanoimprint lithography [19-23]. In this work we have used the nanoimprint lithography method to fabricate the ormocomp nanowire. This method is a top-down process, which can precisely control the dimensions and uniformity of the structure. The nanoimprint technique promises a simpler, less time consuming, and lower cost process compared to other fabrication techniques of polymer nanowires.

This paper consists of three main parts; (i) the design and simulation of the polymer nanowire structure, (ii) the fabrication process, and (iii) the imaging experiment. The ormocomp nanowire is designed to be used as an integrated optics sensor. The structure dimensions of width and height are optimized to achieve maximum sensitivity. The simulation part is used to study the possible mode field and power confinement in the sensing region over the width and operating wavelength. Water is used as a cladding medium in this experimental work. The fabrication part includes the master silica nanowire fabrication and the fabrication of the ormocomp nanowire using the nanoimprint method. Finally, the experimental results focusing on imaging the optical output signal are studied.

## 2. DESIGN AND SIMULATION

### 2.1 Design of nanowires

In this work, nanowires are proposed to be used in an integrated optics sensing application. Therefore, the nanowires are designed to have feed and tapered waveguides attached at their ends. The feed waveguide is later connected to other optical devices, such as an optical coupler, and an interferometer. The tapered waveguide also plays the important role of reducing the power loss when the light couples from the feed waveguide to the small dimension nanowires. Thus, the power of light interacting with the sensing material is enhanced. The design of the nanowire structure and its cross section is shown in Figure 1.

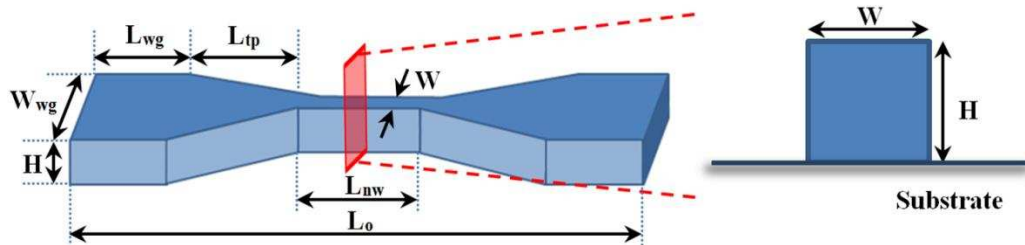


Figure 1: A schematic of the nanowire structure connected with a feed waveguide and a tapered waveguide, and its cross section. The feed waveguide has width  $W_{wg}$ , and length  $L_{wg}$ . The nanowire ( $L_{nw}$ ) with width  $W$  and height  $H$  is attached to the tapered waveguide  $L_{tp}$ . The total length of the nanowire structure ( $L_o$ ) is 5000  $\mu\text{m}$ .

From Figure 1, the integrated nanowire structure consists of the nanowire with length  $L_{nw}$ , the tapered waveguide with length  $L_{tp}=270 \mu\text{m}$  and the feed waveguide with length  $L_{wg}$ . The overall structure has a length of  $L_o=5000 \mu\text{m}$ . The nanowire itself has width ( $W$ ) 0.5  $\mu\text{m}$  to 1.0  $\mu\text{m}$  and height ( $H$ ) 0.5  $\mu\text{m}$ . In this work, the nanowires are designed to have different lengths ( $L_{nw}$ ) in one set. A set of nanowires consists of one reference feed waveguide, one reference tapered waveguide and four different lengths of nanowires which are 250  $\mu\text{m}$ , 500  $\mu\text{m}$ , 1000  $\mu\text{m}$  and 2000  $\mu\text{m}$ . The various lengths of nanowires are used to study the absorption coefficient of the polymer nanowire ( $\alpha_{nw}$ ). The aim of the two reference waveguides is to eliminate the effect of the feed waveguide and the tapered waveguide in the calculation of the absorption coefficient of the nanowires ( $\alpha_{nw}$ ). The set of nanowires containing two reference waveguides and four nanowires is shown in Figure 2.

|                                 |
|---------------------------------|
| (1) $L_{NW} = 2000 \mu\text{m}$ |
| (2) $L_{NW} = 1000 \mu\text{m}$ |
| (3) $L_{NW} = 500 \mu\text{m}$  |
| (4) $L_{NW} = 250 \mu\text{m}$  |
| (5) Tapered waveguide (ref)     |
| (6) Feed waveguide (ref)        |

Figure 2: A designed set of nanowires which consists of four different lengths of nanowires ((1) to (4)), a tapered waveguide reference wire ((5)) and a feed waveguide reference wire ((6)).

The concept behind this sensing application is to have high effective index difference with a small index change. In order to have a high sensitivity nanowire the key parameters that need to be optimized are the width (W) and the height (H) of the nanowires. The variations of the width and height are studied over the effective index and power confinement of the structure as a function of the structure width and the operating wavelength. The ormocomp nanowire ( $n=1.52$ ) is fabricated on glass substrate ( $n=1.45$ ). As in a conventional waveguide, the light is highly confined in the high-index material which is the ormocomp in this case. However, the sensing region is at the interface between the core and the cladding material where the evanescent wave takes place. The change of refractive index of the cladding medium causes the effective index difference. The larger the effective index difference the better the device as far as sensitivity is concerned. Therefore, the parameters are designed in order to enhance the evanescent wave at the boundary of the guiding region and the surrounding medium. The enhancement of the evanescent wave increases the light interaction, and consequently it increases the sensitivity of the device. The cladding material considered in this paper is water ( $n=1.33$ ).

## 2.2 Numerical calculations

To study the behavior of this ormocomp nanowire, the full vectorial H-field finite element formulation [24] has been applied for the modal analysis of the nanowire structure, to determine the propagation characteristics of the fundamental optical mode. There are two methods used in the FEM, the Raleigh-Ritz variational method and the Galerkin method of weighted residuals. In our case, the variational approach is used and the governing differential equation is not solved directly, but the variational expression is formulated as a functional, as shown in Equation 1. The functional used to solve the problems is related to the standard eigenvalue problems, and the modal characterization is obtained by minimizing the functional in Equation 1,

$$\omega^2 = \frac{\int [(\nabla \times \mathbf{H})^* \cdot \varepsilon^{-1} (\nabla \times \mathbf{H}) + p (\nabla \times \mathbf{H})^* (\nabla \times \mathbf{H})] dx dy}{\int \mathbf{H}^* \cdot \mu \mathbf{H} dx dy} \quad (1)$$

where  $\mathbf{H}$  is the full vectorial magnetic field, \* represents a complex conjugate and transpose,  $\omega$  is the angular frequency of the wave,  $\omega^2$  is the eigenvalue, and  $\varepsilon$  and  $\mu$  are the permittivity and permeability respectively.

In this paper, the possible mode fields and power confinement of ormocomp nanowires are studied over the wavelength and the width of the nanowire structure. First, the structure is designed to be a single mode nanowire. Therefore, the nanowire is assumed to have a fixed dimension with the width and height of  $0.5 \mu\text{m}$  and  $1.0 \mu\text{m}$ , respectively. The H-field vector formulation of FEM is used to calculate the modal properties of this waveguide structure by varying the wavelength of excitation. In this case, the cold white light with the operating wavelength between  $400 \text{ nm}$  to  $700 \text{ nm}$  is used as a light source, and the cladding medium is assumed to be water with refractive index of  $1.33$ . With this structure, both the TM mode ( $H_x^{11}$ ) and the TE mode ( $H_y^{11}$ ) are considered. The variation of the effective index of these allowed modes and the power confinement in each region of the nanowire with respect to the operating wavelength are shown in Figure 3a) and Figure 3b) respectively.

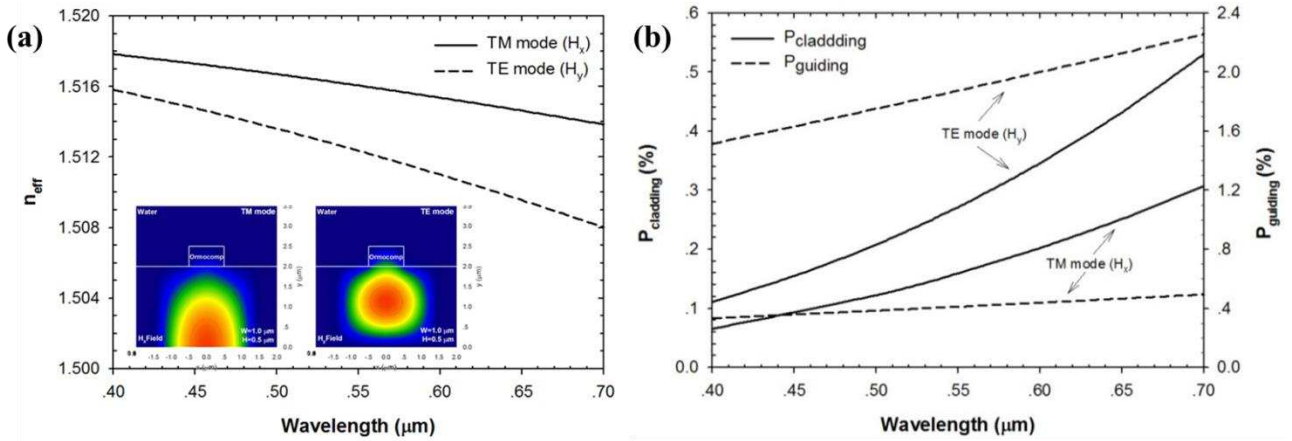


Figure 3: a) The change of effective index over the operating wavelength which is in a visible region for both TM and TE mode. The insets are the mode field profile excited at a wavelength 400 nm of TM (left inset) and TE (right inset) mode in the ormocomp nanowire with 1.0  $\mu\text{m}$  width, and 0.5  $\mu\text{m}$  height. b) The variation of power confinement in the cladding region (sensing region), and the guiding region (ormocomp) with respect to wavelength for TM (10) and TE mode ( $H_y^{11}$ ).

The effective index of the allowed modes is decreased when increasing the wavelength for both TM and TE modes. The graphs in Figure 3a) show that the TM mode has higher effective index compared to the TE mode. The insets in Figure 3a) show the comparison of the fundamental mode field ( $H_x^{11}, H_y^{11}$ ) in the 1.0  $\mu\text{m}$  width and 0.5  $\mu\text{m}$  height ormocomp nanowire. In the TM mode, the optical field is confined more in the substrate whereas the TE mode has a portion of the field confined in the guiding region. Consequently, higher power confinement in both the cladding and the guiding region is obtained in TE mode as shown in Figure 3b). The higher power confinement in the cladding medium, which is water, leads to the higher sensitivity of the nanowires. The power confinement can be enhanced by exciting the optical mode field at a higher operating wavelength. Thus, the 650 nm wavelength (red region) is used as the operating wavelength in the next study to obtain the maximum power confinement possible.

With the fixed operating wavelength of 650 nm (red light source), the effect of the structure width to the allowed mode field and power confinement has been studied, and the results are shown in Figure 4. The study assumed that the structure had height of 0.5  $\mu\text{m}$  and the width was varied from 0.5  $\mu\text{m}$  to 1.0  $\mu\text{m}$ .

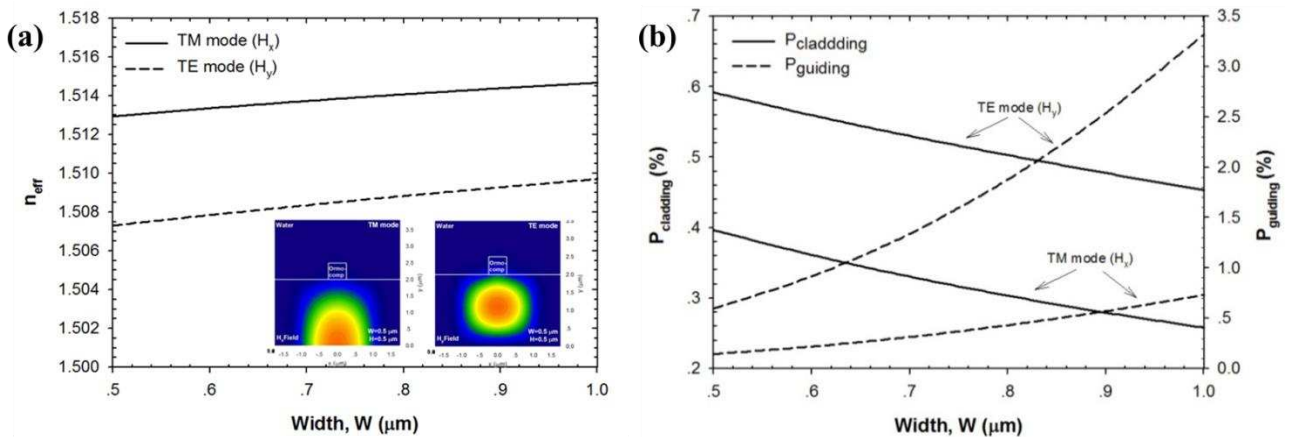


Figure 4: a) The change of effective index over the structure width which is in a range between 0.5  $\mu\text{m}$  and 1.0  $\mu\text{m}$  for both TM and TE modes. The insets show the mode field profile excited at 0.5  $\mu\text{m}$  width nanowire of TM (left inset) and TE (right inset) mode. b) The variation of power confinement in the cladding region (sensing region) and guiding region (ormocomp) with respect to the structure width for TM (10) and TE mode ( $H_y^{11}$ ).

When the structure width is larger, the effective index of the fundamental TM and TE modes are slightly increased. Similarly to the previous results, the TM mode has higher effective index than the TE mode. However, the TE mode has

greater power confinement in both the cladding and the guiding regions compared to the TM mode as presented in Figure 4b). The large nanowire tends to have a small power confinement in the cladding region because there is more volume for the light to be confined in the core region. Hence, the evanescent wave is extended less into the cladding medium, which is the sensing region in our work. The optical mode field profiles for the TM and TE modes are demonstrated in the insets of Figure 4a). The insets show the field in the 0.5  $\mu\text{m}$  width and 0.5  $\mu\text{m}$  height nanowire. Even though the small nanowire provides a higher power confinement in the sensing region and enhances the sensitivity, our work has a limitation in the fabrication process. Therefore, the nanowire with width 1.0  $\mu\text{m}$  and height 0.5  $\mu\text{m}$  is considered in the next section.

### 3. FABRICATION PROCESS

The polymer nanowire is fabricated using the nanoimprint method. It is basically the method to transfer the pattern from the silica master nanowire onto the ormocomp layer. Below, the fabrication process of the silica master and ormocomp nanowires are discussed. As mentioned earlier, the dimensions of the nanowires to be fabricated are fixed at the width of 1.0  $\mu\text{m}$  and height of 0.5  $\mu\text{m}$ . The nanowires are fabricated as a set at different lengths. The four different nanowire lengths are 250  $\mu\text{m}$ , 500  $\mu\text{m}$ , 1000  $\mu\text{m}$ , and 2000  $\mu\text{m}$ . In addition, the feed waveguide and tapered waveguide references are included in the set.

#### 3.1 Silica nanowire fabrication

The ormocomp nanowire can be obtained by transferring the pattern from the silica nanowire. Therefore, the master silica nanowire needs to be a hard mold in the nanoimprint technique. The main fabrication process of silica nanowires includes photolithography and wet etching. The silica nanowires are fabricated on a 6-inch silicon wafer. First, the oxide layer is deposited on the substrate using low pressure chemical vapor deposition (LPCVD) at 1000°C. Then 1.09  $\mu\text{m}$  thickness of sumitomo PFI-34A photoresist is spin-coated on the oxide layer. The pattern of the set of nanowires is transferred onto the photoresist layer by UV exposure for 340 ms. The power of the UV lamp in this treatment is 350.81  $\text{mW}/\text{cm}^2$ . After post-bake at 110°C for 3 mins, the photoresist is developed using tokuyama SD-W for 60 s. The hard bake then needs to harden the photoresist pattern, and prepare it for the next oxide etch. Buffered oxide etch (BOE) is a chemical used to etch the oxide layer. It is a wet etch made of 40% ammonium fluoride ( $\text{NH}_4\text{F}$ ) and 49% hydrofluoric acid (HF) in the volume ratio of 6:1. Finally, piranha solution is used to remove the residual photoresist on the silica nanowire pattern. Piranha is the solution made of 70% sulfuric acid ( $\text{H}_2\text{SO}_4$ ) and 30% hydrogen peroxide ( $\text{H}_2\text{O}_2$ ) in the ratio of 4:1. The fabricated nanowire is shown in Figure 5.

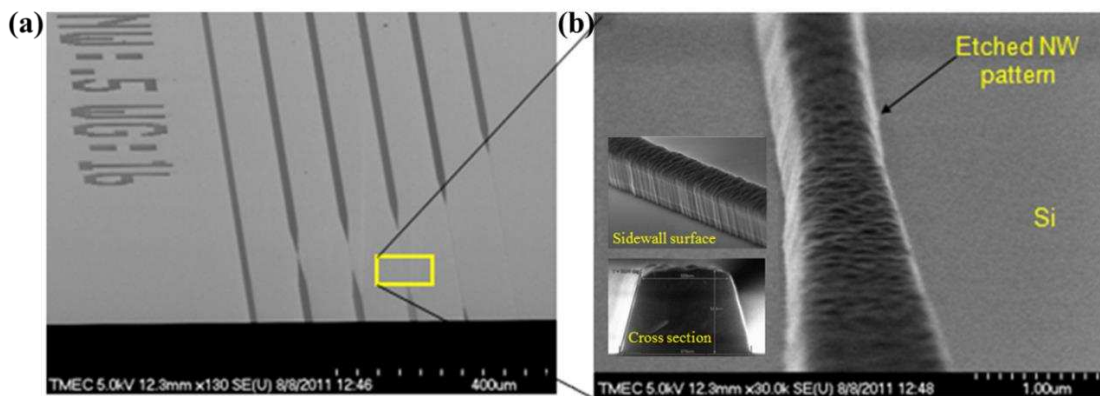


Figure 5: a) SEM image of nanowires in one set including two reference waveguides and four different lengths of nanowires. b) The magnification SEM image at the part of the nanowire involving the sidewall surface and cross section.

The fabricated set of silica nanowires consisting of four different lengths of nanowires and two reference waveguide can be seen in Figure 5a). Figure 5b) shows the magnification part of silica nanowire including the sidewall surface and cross section. The surface roughness is clearly seen in the Figure 5b). Even though, the silica nanowire is designed to have a

vertical sidewall, the wet etching makes the nanowire to have non-vertical sidewalls. Measurements show that the sidewall angle is around  $75^\circ$ .

### 3.2 Ormocomp nanowire fabrication

The polymeric material used to fabricate the polymer nanowire in this work is the ormo-comp. It is a UV curable material for the nanoimprint process with refractive index of 1.52. To perform the nano-imprint process, the nanowire pattern is transferred from the master silica nanowire onto the ormo-comp layer using PDMS (Polydimethylsiloxane). The silica nanowire is considered to be the hard mold whereas the PDMS is considered to be the soft mold in the nanoimprint technique. First, PDMS has to be prepared by mixing the silicone elastomer base and curing agent with the ratio of 7:1 by weight. This ratio can be varied depending on the desired hardness of the PDMS mold. The mixture is then coated on the desired master silica nanowire and goes under the degas process for 30 minutes in order to remove all the bubbles. To harden the PDMS, it is cured at the temperature of  $100^\circ\text{C}$ . After the curing process, the PDMS is removed from the silicon substrate. The pattern created on the PDMS soft mold is the reverse pattern of the silicon nanowire. The process flow to obtain the PDMS soft mold is shown in Figure 6.

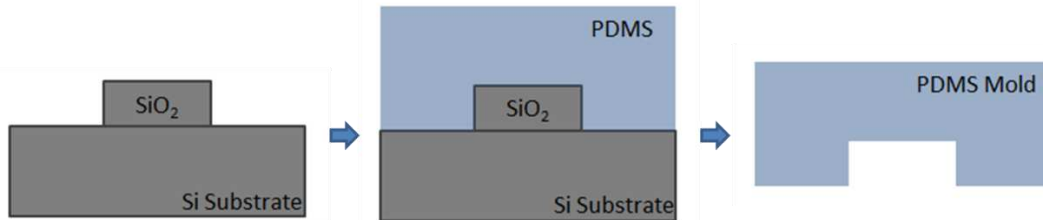


Figure 6: The preparation of PDMS soft mold from the master silica nanowire. The reversed pattern of silica nanowire is obtained in the PDMS soft mold.

The next step is to transfer the pattern from the PDMS soft mold onto the ormo-comp layer. The ormo-comp nanowire is fabricated on a glass slide substrate. First, the ormo-comp is dispensed on the substrate. Next the PDMS mold is used to stamp the nanowire pattern on the ormo-comp layer. Then, the ormo-comp is cured with UV light for 5 minutes. After that the PDMS is removed. The same pattern with the silica hard mold is now appearing on the ormo-comp layer. The nanoimprint process using PDMS stamped on ormo-comp layer is shown in Figure 7.

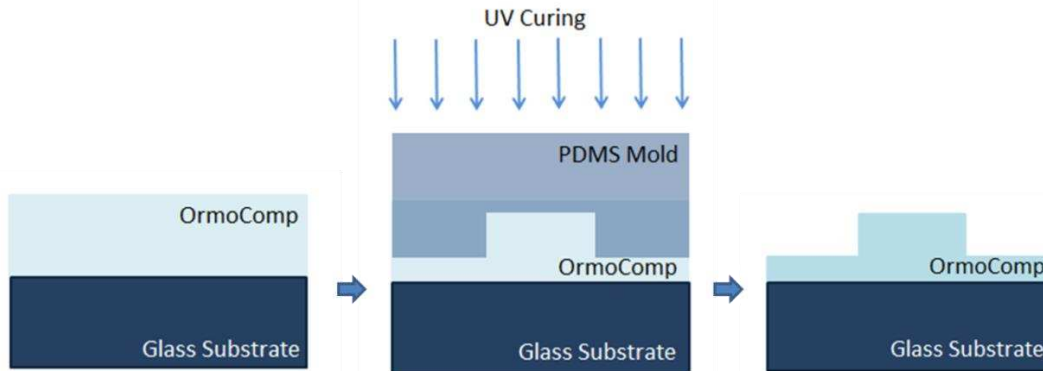


Figure 7: A schematic showing the process flow of the nanoimprint technique used to obtain the ormo-comp nanowire.

However, the fabricated ormo-comp nanowire is considered to be a rib waveguide instead of strip waveguide. This is due to the leftover of ormo-comp layer on the glass substrate. The image of the ormo-comp nanowire obtained from using the nanoimprint technique is shown in Figure 8.

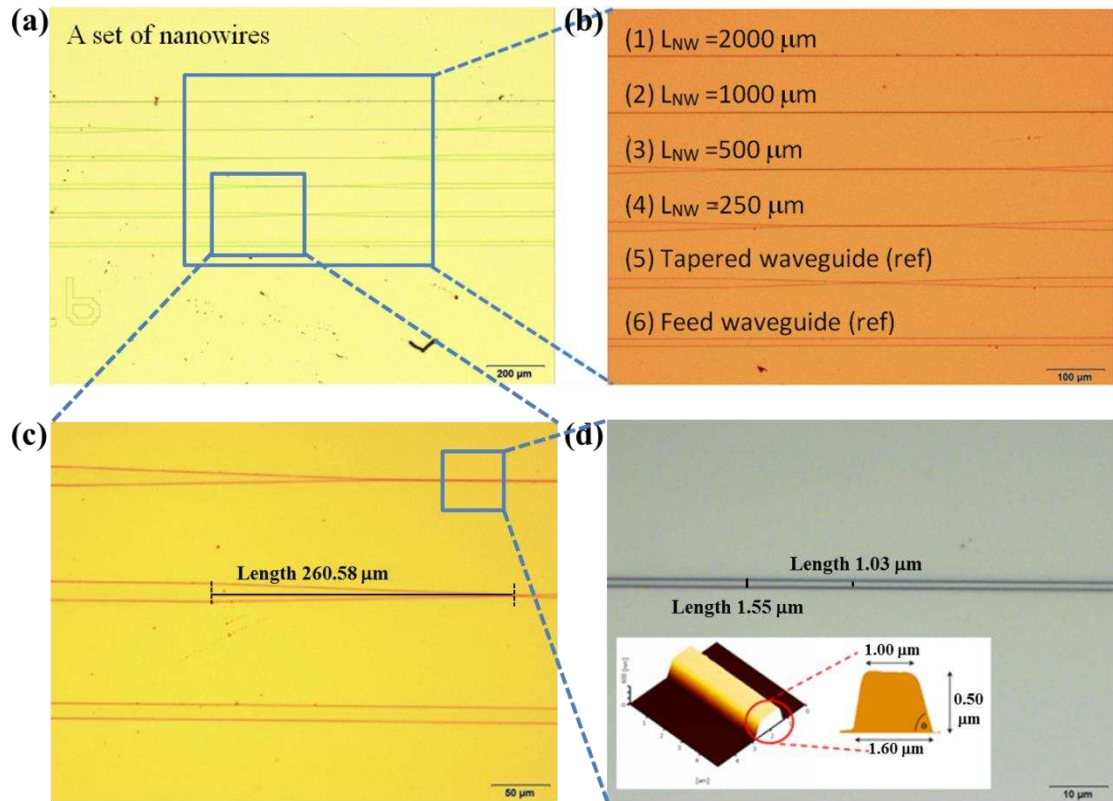


Figure 8: An optical image of a) a set of nanowires, b) larger magnification of the nanowire set consisting of the feed waveguide, the tapered waveguide, and four different lengths of nanowires, c) feed waveguide and tapered waveguide, and d) 1  $\mu\text{m}$  width nanowire. The inset is the AFM image of 1  $\mu\text{m}$  width ormocomp nanowire and its cross section.

The optical microscope images of the ormocomp nanowire at different magnifications are seen in Figure 8. The non-vertical sidewall structure can also be observed from the optical microscope as shown in Figure 8d). The inner width is measured to be 1.03  $\mu\text{m}$ , and the outer width is measured to be around 1.55  $\mu\text{m}$ . This result matches the image obtained from the AFM as shown in the inset. From the AFM, the width at the top surface is 1.0  $\mu\text{m}$  whereas the width at the substrate is 1.6  $\mu\text{m}$ .

#### 4. EXPERIMENTAL RESULTS

In this section we present the results of the experiments performed to image the optical field at the output of the signal guided along the nanowire. The intensity of the output signal is obtained using a computer program. The optical setup to image the signal consists mainly of a red LED light source connected with a single mode optical fiber, the sample stand and two CCD cameras. The light source and the CCD cameras are placed on a xyz stage. The schematic of the optical setup to image the optical output signal is demonstrated in Figure 9.



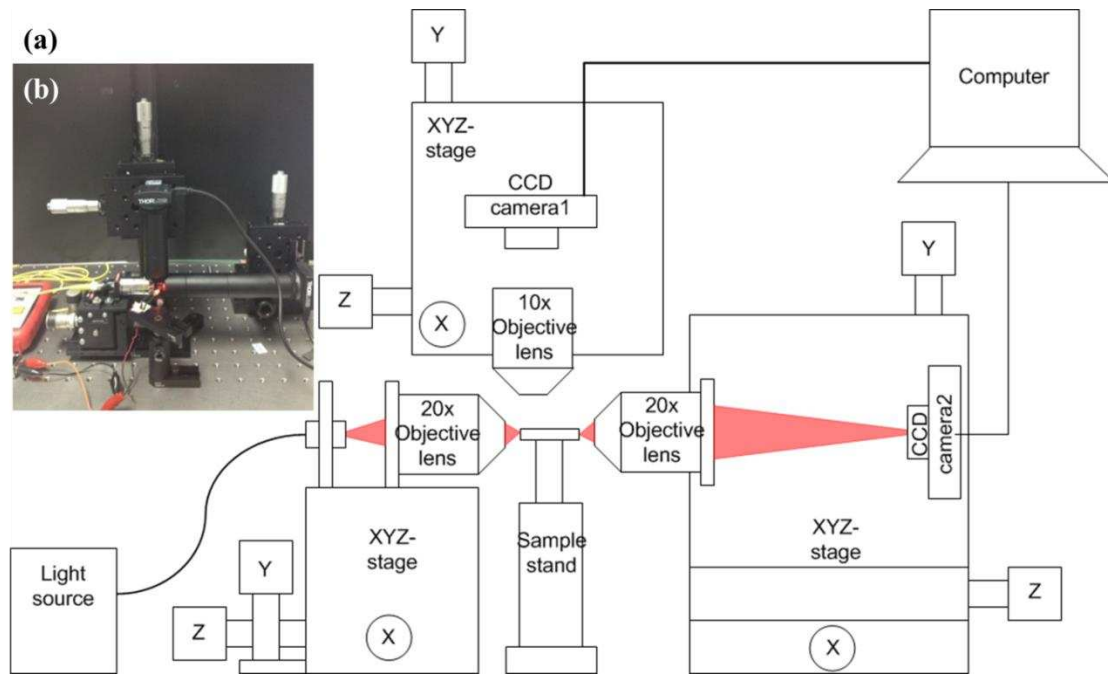


Figure 9: a) A schematic showing the optical setup to image the optical field output signal. b) The actual optical set up.

As shown in Figure 9, the red LED is connected to a single mode optical fiber and it is used as a light source (650 nm). The objective lens with magnification of 20x is used to focus the light, and also enhance the input signal. In an alignment process, the objective lens with the magnification of 10x connected with CCD camera is placed on the top of nanowire stand. It is used to align the optical fiber and the ormocomp nanowire. With the alignment, the focused light is coupled into the specific nanowire, and then propagates along the wire. The output signal is detected by another CCD camera connected with the 20x objective lens which is used to magnify the output image. The image of the optical field output is programmed to extract the intensity. The images and their average intensity of feed waveguide reference and the longest nanowire obtained from the programming are shown in Figure 10a), and Figure 10b), respectively. The actual images obtained from the CCD camera are shown in the insets.

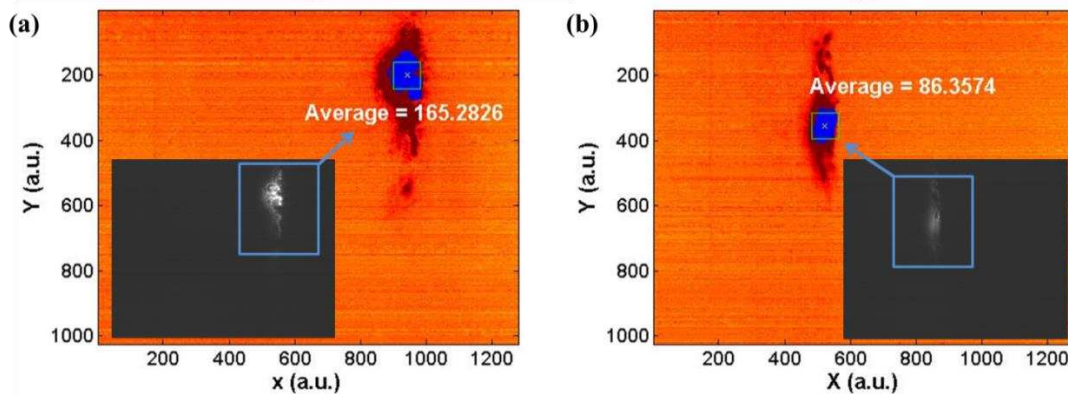


Figure 10: A CCD camera image of the output signal of a) reference waveguide and b) nanowire with the length of 2000  $\mu\text{m}$ .

In order to obtain the average intensity, the highest intensity in the image needs to be found and also locate the point first. After that, the points, where the intensity is more than 70% of the maximum intensity, are located. The high intensity points are scattered. Therefore, the center of scattering is marked, and enclosed by the square boundary. The average intensity is finally calculated from the high intensity located in the boundary. Further experiments are needed to study the scattering effect, the absorption coefficient, and the effect of surface plasmon resonance when the ormocomp nanowire is coated with a metal layer.

## 5. CONCLUSION

In this paper we discussed the study of polymeric ormocomp nanowires including the structure design, the simulation of the possible mode field guided in the nanowire, the fabrication process using the nanoimprint technique and the imaging of the optical output signal. The ormocomp nanowire is designed to be used in an integrated optical sensing application with the maximum possible sensitivity. To enhance the sensitivity, the power confinement in the cladding region has to be maximized. This can be done by optimizing the key parameters of the nanowire structure which is the width in this case. The ormocomp nanowire is designed to have four different lengths which are 250  $\mu\text{m}$ , 500  $\mu\text{m}$ , 1000  $\mu\text{m}$ , and 2000  $\mu\text{m}$ . The optical mode field and the power confinement in the nanowire are studied over the structure width and the operating wavelength in the visible range. The cladding material is water ( $n=1.33$ ). From the simulation results, the small nanowire excited with high operating wavelength (red=650 nm) is the most sensitive structure. However, the optimum parameters are at 1.0  $\mu\text{m}$  width and 0.5  $\mu\text{m}$  height in order to have high power confinement in the sensing region and still be under the fabrication limit. In the fabrication process, the nanoimprint technique is used to transfer the pattern from the silica nanowire onto the ormocomp layer. To image and measure the output signal a CCD camera is used in the optical setup connected to a computer for processing the intensity from the image. The issues of the scattering effect and the absorption coefficient of the ormocomp nanowire will be further studied.

## REFERENCES

- [1] G. Shen, P.-C. Chen, K. Ryu et al., "Devices and chemical sensing applications of metal oxide nanowires," *Journal of Materials Chemistry*, 19(7), 828-839 (2009).
- [2] M. Yun, N. V. Myung, R. P. Vasquez et al., "Nanowire growth for sensor arrays." 37-45.
- [3] C. Themistos, M. Rajarajan, B. M. A. Rahman et al., "Characterization of Silica Nanowires for Optical Sensing," *J. Lightwave Technol.*, 27(24), 5537-5542 (2009).
- [4] D. J. Sirbulu, A. Tao, M. Law et al., "Multifunctional nanowire evanescent wave optical sensors," *Advanced Materials*, 19(1), 61-66 (2006).
- [5] B. MacCraith, V. Ruddy, C. Potter et al., "Optical waveguide sensor using evanescent wave excitation of fluorescent dye in sol-gel glass," *Electronics letters*, 27(14), 1247-1248 (1991).
- [6] J. Lou, L. Tong, and Z. Ye, "Modeling of silica nanowires for optical sensing," *Opt. Express*, 13(6), 2135-2140 (2005).
- [7] J. Wang, and D. Dai, "Highly sensitive Si nanowire-based optical sensor using a Mach-Zehnder interferometer coupled microring," *Optics letters*, 35(24), 4229-4231 (2010).
- [8] J. Wang, S. He, and D. Dai, "Silicon-nanowire-based optical sensor with high sensitivity and large measurement range by using Mach-Zehnder interferometer-coupled microring." 79900V-79900V-6.
- [9] D. Leung, X. Kan, B. Rahman et al., "Optimizing the power confinement in silicon slot waveguides by use of Finite Element Method." 83071A-83071A-6.
- [10] F. Dell'Olio, and V. M. Passaro, "Optical sensing by optimized silicon slot waveguides," *Opt. Express*, 15(8), 4977-4993 (2007).
- [11] N. T. Kemp, D. McGrouther, J. W. Cochrane et al., "Bridging the gap: polymer nanowire devices," *Advanced Materials*, 19(18), 2634-2638 (2007).
- [12] B. Adhikari, and S. Majumdar, "Polymers in sensor applications," *Progress in polymer science*, 29(7), 699-766 (2004).
- [13] J. Huang, S. Virji, B. H. Weiller et al., "Polyaniline nanofibers: facile synthesis and chemical sensors," *Journal of the American Chemical Society*, 125(2), 314-315 (2003).
- [14] H. Liu, J. Kameoka, D. A. Czaplewski et al., "Polymeric Nanowire Chemical Sensor," *Nano letters*, 4(4), 671-675 (2004).
- [15] K. Ramanathan, M. A. Bangar, M. Yun et al., "Bioaffinity sensing using biologically functionalized conducting-polymer nanowire," *Journal of the American Chemical Society*, 127(2), 496-497 (2005).
- [16] H. Fang, D. Yuan, R. Guo et al., "Fabrication of Patterned Polymer Nanowire Arrays," *ACS nano*, 5(2), 1476-1482 (2010).
- [17] F. Gu, L. Zhang, X. Yin et al., "Polymer single-nanowire optical sensors," *Nano letters*, 8(9), 2757-2761 (2008).

- [18] X. Wang, C. Drew, S.-H. Lee et al., "Electrospun nanofibrous membranes for highly sensitive optical sensors," *Nano letters*, 2(11), 1273-1275 (2002).
- [19] H. Lee, B. P. Lee, and P. B. Messersmith, "A reversible wet/dry adhesive inspired by mussels and geckos," *Nature*, 448(7151), 338-341 (2007).
- [20] A. Geim, S. Dubonos, I. Grigorieva et al., "Microfabricated adhesive mimicking gecko foot-hair," *Nature materials*, 2(7), 461-463 (2003).
- [21] J. Liu, Y. Lin, L. Liang et al., "Templateless assembly of molecularly aligned conductive polymer nanowires: a new approach for oriented nanostructures," *Chemistry-A European Journal*, 9(3), 604-611 (2003).
- [22] A. I. Hochbaum, R. Fan, R. He et al., "Controlled growth of Si nanowire arrays for device integration," *Nano letters*, 5(3), 457-460 (2005).
- [23] T. Mårtensson, P. Carlberg, M. Borgström et al., "Nanowire arrays defined by nanoimprint lithography," *Nano letters*, 4(4), 699-702 (2004).
- [24] B. Rahman, and J. Davies, "Finite-element solution of integrated optical waveguides," *Lightwave Technology, Journal of*, 2(5), 682-688 (1984).